High-throughput three-dimensional lithographic microfabrication

Citation: Kim, Daekeun, and Peter T. C. So. "High-Throughput Three-Dimensional Lithographic Microfabrication." Optics Letters 35, no. 10 (May 6, 2010): 1602.

As Published: http://dx.doi.org/10.1364/OL.35.001602

Publisher: The Optical Society

Persistent URL: http://hdl.handle.net/1721.1/120522

Version: Author's final manuscript: final author's manuscript post peer review, without publisher's formatting or copy editing

HHS Public Access

Author manuscript

Opt Lett. Author manuscript; available in PMC 2018 January 20.

Published in final edited form as:

Opt Lett. 2010 May 15; 35(10): 1602–1604.

High-throughput three-dimensional lithographic microfabrication

Daekeun Kim[1] and **Peter T. C. So**[1,2,*]

[1]Department of Mechanical Engineering, Massachusetts Institute of Technology, 77 Massachusetts Avenue, Cambridge, Massachusetts 02139, USA

[2]Department of Biological Engineering, Massachusetts Institute of Technology, 77 Massachusetts Avenue, Cambridge, Massachusetts 02139, USA

Abstract

A 3D lithographic microfabrication process has been developed that is high throughput, scalable, and capable of producing arbitrary patterns. It offers the possibility for industrial scale manufacturing of 3D microdevices such as photonic crystals, tissue engineering scaffolds, and microfluidics chips. This method is based on depth-resolved wide-field illumination by temporally focusing femtosecond light pulses. We characterized the axial resolution of this technique, and the result is consistent with the theoretical prediction. As proof-of-concept experiments, we demonstrated photobleaching of 3D resolved patterns in a fluorescent medium and fabricating 3D microstructures with SU-8 photoresist.

Advanced three-dimensional (3D) microfabrication techniques have been developed with resolutions reaching tens of nanometers [1–4], and a class of notably powerful techniques is based on two-photon excitation (TPE). Two-photon microfabrication attains 3D resolution by spatially focusing excitation light to induce nonlinear excitation within a femtoliter-size volume. This approach has been successfully applied to prototype fabrication including optical storages [5], photonic crystals [6], microfluidic devices [7], smart materials [8], and tissue scaffolds [9]. However, traditional two-photon microfabrication builds 3D structures point-by-point in a sequential fashion; the low fabrication speed prevents its use in high-throughput manufacturing. Other high-speed 3D microfabrication techniques, such as mask-directed two-photon lithography [8,10], multifocal two-photon fabrication [11], proximity field nanopatterning [12], multibeam interferometry [13] and membrane-assisted microtransfer molding [14], can be more difficult to implement or have limited flexibility in making arbitrary 3D structures.

In this Letter, we introduce a high-throughput 3D microfabrication technique analogous to standard photolithography. It is a high-throughput process where nanoscale patterns can be potentially printed in parallel on centimeter-size wafers. One of its important features is scalability; unlike sequential fabrication methods, increasing feature size does not necessarily sacrifice manufacturing speed. It should be noted that typical photolithography is a 2.5D manufacturing technique; 3D structures with limited aspect ratios can be made by

*Corresponding author: ptso@mit.edu.

OCIS codes: 120.4610, 190.4180, 230.4000.

rather labor-intensive process involving repeated rounds of resist coating, exposure, and etching. We demonstrate an extension of photolithographic technique to 3D by temporal-focusing-based wide-field TPE. Temporal focusing was first introduced for microscopic imaging [15,16]. In wide-field excitation, photon flux distribution is spatially uniform. In order to achieve 3D resolution, temporal focusing is implemented by regulating the laser pulse width such that it is minimized at the focal plane.

Figure 1 shows the design of the 3D lithographic microfabrication. A Ti:sapphire femtosecond pulsed laser (Tsunami, Spectra-Physics, Mountain View, California) pumped by a cw diode-pumped solid-state laser (Millennia Xs, Spectra-Physics, Mountain View, California) was used to provide a 80 MHz train of 100 fs pulses at a center wavelength of 780 nm. The $1/e^2$ beam diameter of the ray was about 1–2 mm. The 3D lithographic microfabrication system further consisted of a reflective diffraction grating with groove frequency of 600 grooves/mm (53004BK02-35IR, Richardson Grating Lab, Rochester, New York), a high-NA objective (Fluar, 40×/1.30 Oil, Zeiss MicroImaging, Thornwood, New York), and a customized chrome-coated optical mask (Fine Line Imaging Inc., Colorado Springs, Colorado). The diffraction grating surface and the mask surface were placed at the conjugate planes of the object plane, ensuring that a scaled version of the mask pattern can be produced at the object plane. Away from the focal plane, this arrangement guaranteed that the different spectral components dispersed by the grating were separated spatially, resulting in broader pulse width and lower TPE efficiency due to the constancy of the time–bandwidth product. At the focal plane, the different spectral components were recombined, the pulse width was minimized, and TPE efficiency was maximized. Fabrication was accomplished by printing one layer at a time. After the pattern at a given plane was fabricated, the objective was moved to the next axial position by using a piezo-positioner (MI-POS500, piezosystem jena Inc., Hopedale, Mass.), the mask pattern was updated, and the next layer was ready for printing. Repeating this process resulted in a layer-by-layer generated 3D microstructure. The patterns on the optical mask were projected on the focal plane with an effective demagnification of 60, and the fabrication area on the specimen was approximately 35 μm × 24 μm.

While it is easy to measure lateral fabrication resolution with microfabrication, it is more difficult to evaluate axial fabrication resolution, since micrometer-scale features cannot be located without supporting structures in 3D. We developed a fluorescence-based evaluation approach by using a photobleaching process. Photobleaching has been proposed as a mechanism to build 3D memory storage [17] and can serve as a partial model of microfabrication processes such as photopolymerization where chemical interaction with reactive oxygen species is also important [18,19]. For the fluorescent substrate, 15 μm diameter yellow-green (505/515) fluorescent polystyrene microspheres (F-8844, Invitrogen, Carlsbad, Calif.), uniformly labeled with fluorophores, were selected. To evaluate the axial fabrication resolution, a region at the center of the microsphere was photobleached, and the resultant pattern was imaged by using a standard point-scanning two-photon microscope. Axial intensity profile was averaged laterally in the photobleached area and converted to an effective axial point spread function (PSF), which is defined as a convolution of the printing PSF and the reading PSF. Embedding medium selection and absorption energy dose control are critical for obtaining a diffraction-limited PSF; their effects on the PSF are presented in

Fig. 2(a). With an illumination power of 280 mW at the objective, it is important to limit the exposure time to prevent overexposure, which results in PSF broadening. Additionally, the embedding medium around the microsphere should be carefully selected to avoid a lensing effect induced by refractive index (RI) mismatch at the microsphere–medium interface. As expected, larger RI mismatch resulted in greater PSF degradation. By optimizing embedding medium RI and exposure time, diffraction-limited axial fabrication resolution can be achieved as shown in Fig. 2(b) and is in good agreement with theoretical calculations not presented here. For photopolymerization, features below the diffraction limit may be produced due to the presence of a threshold energy level below which polymerization cannot be initiated [20]. As a proof-of-concept study, 3D microprinting based on photobleaching was demonstrated. Figure 3(a) explains how depth-resolved micropatterns were printed in the fluorescent microsphere; each symbol in the MIT logo was photobleached at the designated depth with 5 μm axial separation in the microsphere. During the printing process, 280 mW average laser power at the objective and 20 s exposure time were applied for each symbol. Figure 3(b) shows the fluorescence images of the printed symbols acquired with a standard two-photon microscope. Each symbol was clearly identified at its corresponding depth. There is a small crosstalk among layers, but it is expected to be less critical for photopolymerization process where there exists an intensity threshold for activation. Last, this technique was applied to 3D microfabrication with SU-8 photoresist (SU-8 2010, MicroChem Corp., Newton, Mass.). A standard SU-8 manufacturing process [21] was employed except for the exposure procedure. High-aspect-ratio (1:5) symbols for the MIT logo were constructed and are shown in Fig. 4. The time required to write each symbol was of the order of seconds.

In conclusion, we have conceived and implemented a 3D lithographic microfabrication system. We have validated that its diffraction-limited printing resolution can be achieved and further demonstrated printing capability of 3D-resolved micropatterns at multiple depths through a photobleaching process. By building 3D SU-8 microstructures, we have demonstrated 3D microfabrication. We believe that this novel microfabrication technique has many potential manufacturing applications after several technological hurdles are overcome. First, despite its scalable capability, our fabrication area is limited by the available peak power in a typical Ti:sapphire oscillator. Given the quadratic power dependence of TPE, the illumination beam can project onto a significantly large area at a time by using higher peak power light sources such as a regenerative amplifier. It should also be noted that the optical power and the field of view in the selection of standard commercial objectives confines maximum lithography area with micrometer-scale 3D features, and it demands customized large field-of-view high-NA objective. Second, the microfabrication speed is further restricted by low two-photon absorption of many standard photoinitiators, and the commercialization of high two-photon cross-section photoinitiators is clearly a priority [22,23]. Third, while sequential insertion of different optical masks at different planes is sufficient for conceptual demonstration, the incorporation of a high-bandwidth configurable optical mask generator based on a digital mirror array or spatial light modulator will further improve microfabrication throughput. With these enhancements, we expect that applications of this innovative microfabrication scheme will not only allow the prototypical 3D microstructures in the research but may also enable their industrial scale production.

Acknowledgments

This work was supported by the MIT Deshpande Center for Technological Innovation and Singapore–MIT Alliance for Research and Technology (SMART).

References

1. Hatzor A, Weiss PS. Science. 2001; 291:1019. [PubMed: 11161210]
2. Kawata S, Sun HB, Tanaka T, Takada K. Nature. 2001; 412:697. [PubMed: 11507627]
3. Piner RD, Zhu J, Xu F, Hong SH, Mirkin CA. Science. 1999; 283:661. [PubMed: 9924019]
4. Tseng AA. Small. 2005; 1:924. [PubMed: 17193371]
5. Cumpston BH, Ananthavel SP, Barlow S, Dyer DL, Ehrlich JE, Erskine LL, Heikal AA, Kuebler SM, Lee IYS, McCord-Maughon D, Qin JQ, Rockel H, Rumi M, Wu XL, Marder SR, Perry JW. Nature. 1999; 398:51.
6. Sun HB, Xu Y, Juodkazis S, Sun K, Watanabe M, Matsuo S, Misawa H, Nishii J. Opt Lett. 2001; 26:325. [PubMed: 18040312]
7. Stoneman M, Fox M, Zeng CY, Raicu V. Lab Chip. 2009; 9:819. [PubMed: 19255664]
8. Kaehr B, Shear JB. Proc Natl Acad Sci USA. 2008; 105:8850. [PubMed: 18579775]
9. Cunningham LP, Veilleux MP, Campagnola PJ. Opt Express. 2006; 14:8613. [PubMed: 19529241]
10. Kaehr B, Shear JB. J Am Chem Soc. 2007; 129:1904. [PubMed: 17260997]
11. Kato J, Takeyasu N, Adachi Y, Sun HB, Kawata S. Appl Phys Lett. 2005; 86:044102.
12. Jeon S, Malyarchuk V, Rogers JA, Wiederrecht GP. Opt Express. 2006; 14:2300. [PubMed: 19503567]
13. Shoji S, Kawata S. Appl Phys Lett. 2000; 76:2668.
14. LaFratta CN, Li LJ, Fourkas JT. Proc Natl Acad Sci USA. 2006; 103:8589. [PubMed: 16720698]
15. Oron D, Tal E, Silberberg Y. Opt Express. 2005; 13:1468. [PubMed: 19495022]
16. Zhu GH, van Howe J, Durst M, Zipfel W, Xu C. Opt Express. 2005; 13:2153. [PubMed: 19495103]
17. Pudavar HE, Joshi MP, Prasad PN, Reinhardt BA. Appl Phys Lett. 1999; 74:1338.
18. Diaspro, A., Chirico, G., Usai, C., Ramoino, P., Dobrucki, J. Handbook of Biological Confocal Microscopy. 3rd. Pawley, JB., editor. Springer; 2006. p. 690-702.
19. Farrell TJ, Hawkes RP, Patterson MS, Wilson BC. Appl Opt. 1998; 37:7168. [PubMed: 18301543]
20. Sun HB, Kawakami T, Xu Y, Ye JY, Matuso S, Misawa H, Miwa M, Kaneko R. Opt Lett. 2000; 25:1110. [PubMed: 18064287]
21. Processing Guidelines for SU-8 2010. MicroChem Corp; Newton:
22. Rumi M, Ehrlich JE, Heikal AA, Perry JW, Barlow S, Hu ZY, McCord-Maughon D, Parker TC, Rockel H, Thayumanavan S, Marder SR, Beljonne D, Bredas JL. J Am Chem Soc. 2000; 122:9500.
23. Haske W, Chen VW, Hales JM, Dong WT, Barlow S, Marder SR, Perry JW. Opt Express. 2007; 15:3426. [PubMed: 19532584]

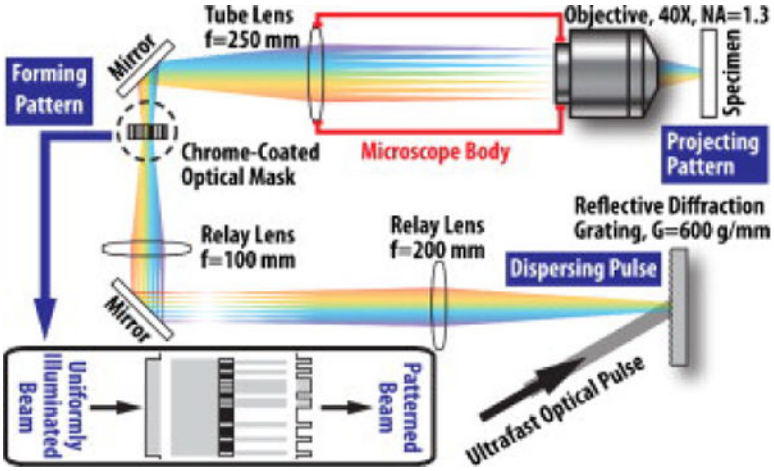

Fig. 1.

(Color online) Schematic diagram of 3D lithographic microfabrication system. Inset, how planar pattern is created through the optical mask.

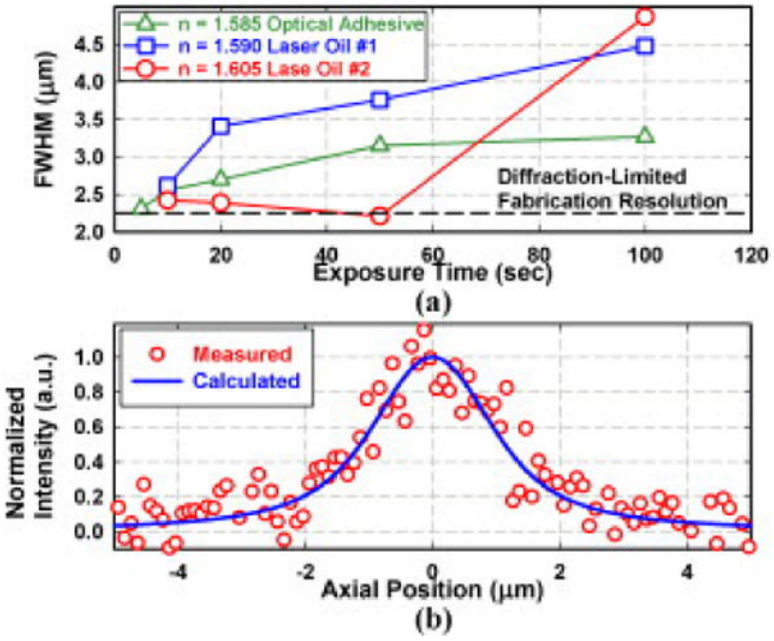

Fig. 2.

(Color online) Effective axial PSF: (a) FWHM of the effective axial PSF as a function of different exposure times and embedding media. (b) Circles, the measured effective axial PSF (with laser oil 2, exposure time of 50 s) has a FWHM of 2.27 μm (solid curve). The predicted effective axial PSF is obtained from convolving the theoretical printing and reading PSFs with FWHMs of 1.65 and 1.16 μm, respectively.

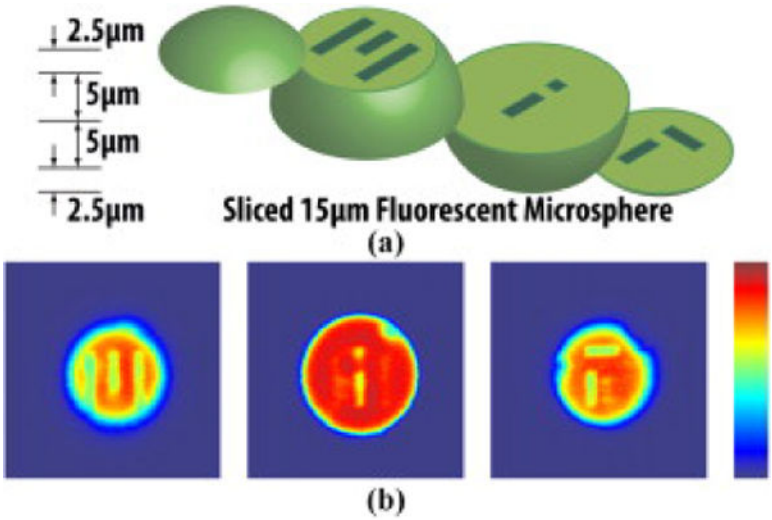

Fig. 3.

(Color online) 3D depth-resolved pattern generation by photobleaching inside a microsphere: (a) Pictorial illustration of 3D microprinting of MIT logo at different depths: ‘M’ at top, ‘I’ at middle, ‘T’ at bottom. (b) Reading patterns at different layers. From left to right, 5 μm above center, at the center, and 5 μm below center.

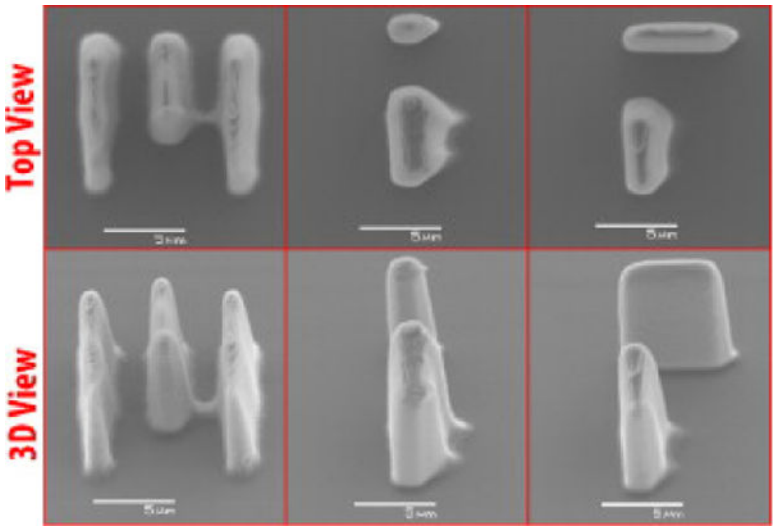

Fig. 4.

(Color online) Scanning electron microscopy images of 3D microfabrication of MIT logo made of SU-8 photoresist.